

In Situ Corrosion Measurements and Management of Shipwreck Sites

IAN D. MACLEOD

INTRODUCTION: CORROSION PHENOMENA AND IRON SHIPWRECKS

The overall impression of an iron shipwreck site is often dominated by the remains of the boiler, engine, and frames that once gave the vessel its form. In warm tropical to subtropical seawater, corroding iron and steel rapidly become encapsulated by encrusting organisms such as coralline algae and bryozoa (North, 1976). This encapsulation begins the process of separating the anodic and cathodic sites of the corrosion cell, with oxygen reduction generally happening on the outer surface and oxidation of the metal occurring underneath the marine growth (MacLeod, 1989a). Under such conditions, the cathodic reduction of dissolved oxygen is the rate-determining step in the overall corrosion process.

The main environmental parameters controlling the level of dissolved oxygen are salinity and water temperature. Colder sites, and those with lower salinity, will normally have greater amounts of dissolved oxygen in the waters surrounding the wreck. Since

Ian D. MacLeod, Director, Museum Services, Western Australian Museum, Fremantle, Western Australia WA 6160.

International Handbook of Underwater Archaeology, edited by Carol V. Ruppé and Janet F. Barstad. Kluwer Academic/Plenum Publishers, New York, 2002.

metal ions are produced during the corrosion process, the positive charges released into the immediate environment of the metal surface attract chloride ions through the marine growth. The buildup of chloride ions, from inward diffusion or from the sea, leaves the excavated artifacts at great risk of subsequent corrosion.

Embayed waters and those in cooler regions are dominated by different colonizing marine organisms. In the absence of calcareous colonizing organisms, a corroding iron wreck generally will be covered with a matrix of corrosion products and marine organisms such as algae, barnacles, and tunicates. The wreck *City of Launceston* (1865) in Port Phillip Bay, Australia, typifies such sites. The only major difference in the corrosion processes are the less dense the marine cover, the less the underlying metal is protected from the ravages of dissolved oxygen (MacLeod, 1993a, 1999). Studies on submerged and riparian sites on the River Murray have confirmed that cathodic reduction of dissolved oxygen is the dominant process in determining the overall rate of corrosion (MacLeod, 1994).

Naturally, corrosion rates are dependent on a range of microenvironmental parameters. For iron materials lying above or on the seabed, the primary cathodic reaction is the reduction of dissolved oxygen. For metal totally buried in the sediment and not electrically connected to iron exposed to oxygenated waters, the major cathodic reaction is the reduction of water and the associated evolution of hydrogen. Under such circumstances, the corrosion process is often dominated by microbiological activity (Fischer, 1983) since the presence of dehydrogenase enzymes will often control the rate of hydrogen evolution (Sequeira and Tiller, 1988).

Since the concretion acts as a semipermeable membrane, 100 years of corrosion results in the establishment of a substantially different microenvironment around the metal itself, compared with the surrounding sea. For example, chloride concentration can be increased by a factor of 3 above the mean seawater levels, and pH can fall from the normal value of 8.2 to as low as 4.2 (MacLeod, 1989b). If the matrix of corrosion products and calcareous deposits is accidentally removed, the increased access to oxygen results in accelerated corrosion of iron in a chloride-rich, acidic microenvironment and the loss of archaeological values (MacLeod, 1981, 1987).

On an iron wreck, any nonferrous materials electrically connected to metallic iron will be protected by galvanic coupling. As a result, all copper, brass, and bronze fittings become covered with a thin, adherent, white calcareous concretion (MacLeod, 1982). Once the concretion has formed, the surface is no longer biologically toxic; it is then subject to the normal colonization mechanisms associated with the particular marine ecology of the area.

A novel form of corrosion has been observed on historic shipwrecks where the deleterious effects of galvanic coupling on the corrosion of iron materials are observed where there has been no direct physical contact. This phenomena is now known as *proximity corrosion* and has been observed on the historic shipwreck sites of *Rapid* (1811) and *Hadda* (1877) in Western Australia. These wrecks are in shallow waters at depths of 7 m and 4–6 m respectively. Initial research into the nature of this type of corrosion and its implications for structures has been reported by North (1989).

CORROSION SURVEYS

Routine measurement of electrochemical parameters such as the surface pH of degrading artifacts and the corrosion potential, E_{corr} , of metal objects on wreck sites has a recent

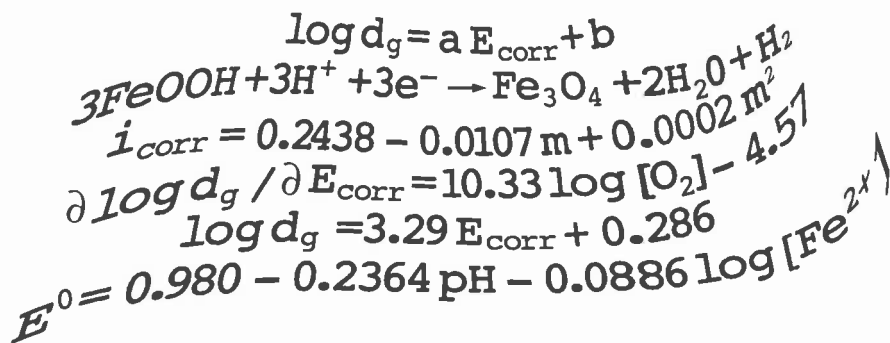


Figure 41.1. Corrosion measurement equations.

history (Lenihan, 1989; MacLeod 1981; North, 1982). Corrosion scientists have found that knowledge obtained through these on-site measurements is an invaluable aid in understanding the corrosion mechanisms and modes of deterioration of materials on archaeological sites.

Corrosion potentials are measured by noting the voltage difference between a platinum electrode in contact with the corroding metal and an appropriate reference electrode. For practical reasons, the digital multimeter is normally housed in a waterproof case, with the electrodes connected via insulated wires sealed through the box with O-rings. A suitable reference electrode for working in open sea water is a silver/silver chloride (Ag/AgCl). If work is done in sediments or in waters subject to sulphide contamination, this double-junction Ag/AgCl electrode is necessary to prevent contamination of the electrode, which would change the standard voltage. Platinum is used as the working electrode because it is chemically inert; the measured voltages refer to the object itself and are not due in part to the nature of the electrode material.

Corrosion potential measurements are made by drilling through the marine growth and placing the platinum electrode into the hole with the reference electrode adjacent to the point of measurement, then reading the voltage. Correct determination of the corrosion potential is normally indicated by a very steady voltage, i.e. a reading that varies by only 1–2 mv over several minutes. The significance of the corrosion potential is that it is a readily measurable parameter sensitive to the rate of metal corrosion. The primary corrosion product occurring underneath the concretion is ferrous chloride (FeCl₂), which subsequently undergoes hydrolysis to {Fe(OH)₂·FeCl₂}. As the ferrous chloride solution diffuses out through the concretion matrix and undergoes hydrolysis, the resulting increase in acidity causes dissolution of calcium carbonate in the encapsulated marine organisms. Reprecipitation of iron carbonate follows with concomitant oxidation of the iron II (Fe²⁺) corrosion products to iron III (Fe³⁺).

SITE-SPECIFIC CORROSION RATES AND USE OF E_{corr}

Archaeologists have a strong desire to determine the long-term rate of deterioration of a shipwreck site. Secondary to this key issue is the desire to understand how the rate of decay changes with the effect of excavation activities or with natural scouring processes associated with heavy storms. Fortunately, historic shipwrecks generally have a unique

record of the effect of corrosion preserved in corroded cast iron objects. For wooden ships, the presence of cast iron cannon provides a source of such data, while for iron shipwrecks, the massive cast iron bollards, capstans, and engine mountings provide a site-specific corrosion database. Because of its elemental composition and associated microstructure, cast iron corrodes to leave behind the original surface dimensions of an object because of its high carbon content. This change results in a composition profile that leaves graphite on the original surface, followed by a mixture of graphite and cementite (Fe_3C , iron carbide), pearlite (a phase consisting of lamellae of cementite and pure iron, or ferrite), and ferrite itself. By drilling into the corroded metal, perpendicular to the exposed face, the researcher can obtain a corrosion profile of the vessel since it was immersed in sea water. Once the drill bit encounters solid material, in the form of uncorroded metal, the penetration depth can be recorded with a micrometer. Penetration depth, or graphitization, of cast iron is a good indicator of the net effects of exposure to the corrosive environments over past centuries.

Previous work has established a direct relationship between the logarithm of the annual rate of corrosion rate of cast iron artifacts and their in situ corrosion potential (MacLeod, 1989a). Annualized corrosion rate is determined by dividing the depth of graphitization d_g by the number of years of the object's immersion; corrosion rates are reported in mm/year. It is desirable to have a number of sets of measurements of depths of graphitization and E_{corr} so that a measure of the variability of data across the site can be determined. Sufficient data has been recorded from a number of sites to ascertain that objects that do not "lie on the straight line" relationship are more than likely to be indicators of significant changes in the nature of the microenvironment since the initial wrecking event.

Site-specific corrosion equations take the general form of Equation 1:

$$\log d_g = a E_{corr} + b \quad (1)$$

where a is a constant for the site at the time of measurement, and b is another constant relating to the general corrosivity of the site. The value of the slope a has been found to be sensitive to temperature and salinity, since these are the two parameters that ultimately determine saturation values of dissolved oxygen in the water. The units of a are volt^{-1} , the reciprocal of this slope provides a measure of the number of volts or millivolts needed per tenfold change in corrosion rate. The higher the dissolved oxygen values, the greater the increase in corrosion rate per unit increase in the value of the corrosion potential.

GENERAL CORROSION PHENOMENA AND USE OF IN SITU CORROSION MEASUREMENTS TO ASCERTAIN RATES OF DECAY

Corrosion potential (E_{corr}) data collected from a number of wreck sites show that archaeological iron is often in strongly reducing conditions, with Eh values at -0.290 ± 0.015 volts at a mean pH of 4.8, or just below the hydrogen evolution potential for that acidity level. Hydrogen has been identified as a major component of gases released when concretions are penetrated for the first time in centuries (MacLeod, 1988). Among the other gases were carbon dioxide (from acid dissolution of calcite and aragonite as a result of hydrolysis reactions) and methane. Analysis of the carbon isotope ratios of $^{13}\text{C}/^{12}\text{C}$

in the methane gave an isotope shift of -4.7 ppt, showing that the methane was inorganically derived via reactions such as those shown in Equation 2:



Since bacteria effectively fractionate carbon isotopes in favor of ^{12}C , an isotope shift ($\delta^{13}\text{C}$) with a value in the range of -55 to -75 ppt (relative to standard limestone, PDB) would be observed for bacterially-produced methane (Hunt, 1979). Inspection of the carbon Pourbaix diagram shows that methane is the thermo-dynamically stable form of carbon under the lower portion of the range of Eh and pH (Pourbaix, 1974) recorded on wreck sites at depths to 22 m.

EFFECTS OF CORROSION PROCESS

Dissolved Oxygen

The equation connecting dissolved oxygen content of seawater and values of a was developed empirically from the following observations. The wreck of the *Lively* (c. 1820), in the warm tropical waters of the Rowley Shoals some 400 km off the Western Australian coast, had a slope of 2.84 (Carpenter and MacLeod, 1993); the average slope of more temperate Australia sites was 3.05; and the much cooler Scottish waters in the Sound of Mull (Ellett and Edwards, 1983) gave a slope of 3.70. Concentration of dissolved oxygen increases as both temperature and salinity fall (Riley and Skirrow, 1975). From a knowledge of salinity and temperatures of wreck sites, it is possible to gain typical values of dissolved oxygen concentration. When the values of the slope a are plotted as a function of the O_2 concentration, the observed slopes were related by Equation 3:

$$\partial \log d_g / \partial E_{corr} = 10.33 \log[\text{O}_2] - 4.57 \quad (3)$$

where the concentration of oxygen is recorded in $\text{cm}^3 \cdot \text{dm}^{-3}$. Once the salinity and temperature of the seawater and hence the dissolved oxygen concentration is known, Equation 3 can be used to calculate the a value for Equation 1. This means that it is now possible to determine the differences in the rates of corrosion for artifacts in similar chemical environments. At least one set of data on $\log d_g$ is needed to determine the value of the constant b in Equation 1 to allow a quantitative calculation of corrosion rates.

As already noted, it is possible to use the shift in E_{corr} values to determine the extent to which a corrosion environment has changed. Once the value of a is known, it is possible to see how many millivolts difference in the value of E_{corr} is needed for a tenfold change in corrosion rates. The *Tafel* slope is the number of millivolts that equates to a tenfold change in corrosion rate (Kiss, 1988). Changes in E_{corr} values, as measured in volts, can then be multiplied by the value of the slope a , and the "multiplier effect" on the corrosion rate is determined by taking the antilogarithm of this value. To determine when any changes in the values of E_{corr} are significant, it is vital to know the reproducibility of data over several seasons. Repeated visits to the SS *Xantho* site showed that the corrosion potential measurements of the boiler were reproducible within ± 2 mV (MacLeod, 1992). If there are larger differences in corrosion potentials, it is possible to state that a change occurred. A change of 3 mV in the value of E_{corr} equates to a variation of 2.5 percent in the cooler Scottish waters off the Isle of Mull, to 1.6 percent in the tropical waters at the *Lively* site in tropical Western Australia.

Cyclic Burial and Exposure

The effects of cyclical burial and exposure of wreck materials and effects on corrosion mechanisms is best illustrated by analysis of SS *Xantho*, which sank off Port Gregory, Western Australia in 1872. A copper wire in an engine room water cooling device showed a number of corrosion layers. When the logarithm of the spacings between the layers was plotted against the number of growth rings, a series of linear relationships showed that the corrosion phenomena on the SS *Xantho* site can be described in terms of *liesegang* phenomena, i.e., of periodic precipitation (MacLeod, 1986). Precipitation of copper sulphides as corrosion products occurs with the change of the microenvironment from aerobic, when the object was exposed to strongly flowing seawater, to anaerobic, when 2 m of sand were deposited on the site. During periods of exposure to open seawater, the fitting was in a passive corrosion state and suffered negligible corrosion. Under anaerobic conditions, the passivating nature of the Cu_2O film was rendered inactive, and significant corrosion took place each time the site was reburied. With 16 corrosion bands over the 113 years since the vessel sank, the data strongly supports a seven-year cycle of burial and exposure. This phenomena readily explains the “newness” of the biological environment on the wreck site, compared with the surrounding reef that was noted during the predisturbance survey (MacLeod et al., 1986).

Water Depth

During the initial corrosion surveys on the wreck site of HMS *Sirius* (1790) on Norfolk Island, it was noted that the cast iron ballast pigs were much more extensively corroded in shallow waters than in the deeper part of the site (MacLeod, 1989a). These differences occurred over the range of water depth from 1.5 to 3.5 m at the high-water mark. Any diver working the site can vouch for major differences in the degree of difficulty of working in the strong surge in the extremely shallow site. Since water depth made such a huge difference to the divers, it is not surprising to find such issues reflected by the degree of degradation of the artifacts. For many years, the search for a model was fruitless, until a larger number of wrecks had been surveyed and their corrosion characteristics noted.

One of the most direct corrosion indices is the annualized depth of corrosion as measured by the mm/year of graphitization of cast iron; this has been plotted as a function of water depth across the site. This research is entirely empirical in nature, and the interpretation of data is subject to change as more sites are examined and the model is refined.

Despite these limitations, some general comments can be made. The shallowest vessel from which data was collected is that of the breastwork monitor HMVS *Cerberus* (1876) in Port Phillip Bay in Victoria, which was sunk as a breakwater in 1926. The deepest vessel is *City of Launceston* (1865) at a depth of 22 m in the middle of the west shipping channel in Port Phillip Bay. The zero water depth for corrosion measurements on *Cerberus* related to the former splash zone, which subsided a few years ago to lie 1 m below its previous level. The annual corrosion rate of 0.242 mm/year at zero water depth relates to the armor plating on the outerdecks of the vessel (MacLeod, 1996a).

Since previous studies had shown that E_{corr} steadily decreased with water depth, the corrosion rates from the iron shipwrecks were plotted according to average water depth.

The best fit for the regression analysis was a quadratic equation (see Equation 4), with the square of the correlation coefficient being 0.9985, a strong indicator that the relationship has a high degree of validity.

$$i_{corr} = 0.2438 - 0.0107 m + 0.0002 m^2 \quad (4)$$

where i_{corr} is in units of mm/year and water depth m is in meters. This equation can be used to calculate the long-term corrosion rate of an iron shipwreck in the open ocean waters of southern Australian latitudes with only water depth being known. The benefit of this relationship is that it can be used by anyone to calculate the expected corrosion rate for vessels when the only archaeological information known is the date of wrecking and water depth. If the original thickness of metal ribs, frames, and plates are known, Equation 4 can be used to estimate how much of the materials is likely to remain on the site (MacLeod, 1998b).

Since corrosion rate decreases in a primarily linear fashion with depth but is corrected for this by a smaller positive term associated with the square of water depth, there comes a point where the corrosion rate will be independent of depth. This minimum, or point of independence from depth, can be determined by differentiation of Equation 4 with regard to the water depth m which gives Equation 5:

$$\partial I / \partial m = 0.0004 m - 0.0107 \quad (5)$$

The minimum value is reached when the slope is equal to zero; this occurs at a water depth of 26.8 m. This observation is profound, implying as it does that, once an iron wreck is in water of greater depth than 26.8 m, the overall effect of the increased depth is limited. *It must be emphasized that these observations are limited to the data collected and that the deepest site measured was 22 m.*

The other implication is that the minimum corrosion rate of iron shipwrecks is 0.100 mm/year, the average long-term corrosion rate of marine iron in an exposed location (La Que, 1975). More experimental data needs to be obtained from deeper water sites to determine how this relationship applies. Given that the general mixing of ocean waters becomes significantly less at depths greater than 35 m (Riley and Skirrow, 1975), other variables are likely to affect the amount of water movement, such as deep ocean currents, that would begin to play a significant role in the supply of dissolved oxygen to the corroding metal surfaces.

Shelter from Prevailing Weather

The effect on overall corrosion rate of an iron shipwreck lying in the lee of an island can now be calculated using Equation 4 to predict the annual rate of decay and by comparing it with the in situ data. A convenient case is that of *Songvaar* (1912), which lies in the lee of Wardang Island in Spencer Gulf, South Australia. The actual corrosion rate of the iron clipper is some 30 percent less than would be anticipated on the basis of the water depth. Another possible factor that may have lowered the historical corrosion rate of *Songvaar* is that, when it sank on its own anchor, the vessel was fully laden with wheat. As the wheat swelled, it would have begun to undergo marked biodeterioration, which would have rendered the waters on the inside of the vessel anaerobic and so reduced the initial corrosion rate. More data from other protected wreck sites is needed before the relative effect of the cargo and the shelter of the island can be quantified.

Explosives

Management of historic shipwrecks without the assistance of enacted protective legislation is made much more difficult by the activities of would-be salvors who attack vessels with explosive charges. Reasons for such vandalism are many but include those of recovery of nonferrous metal fittings for scrap value. An example of the effect of explosives on an historic iron shipwreck can be judged from the wreck of *Clan Ranald* (1909), which sank off Troubridge Point, Gulf St. Vincent, South Australia. If Equation 4 is used to calculate the anticipated corrosion rate, actual data shows an increase of 33 percent above the level based on water depth of 18 m. The increased corrosion rate is probably due to extensive blasting of the site during a series of salvage operations. Shock waves from the exploding charges tend to strip the protective concretion from the hull and other fittings and give the dissolved oxygen direct access to the degraded metal. Observations of the rapid increase in corrosion potential of several hundred millivolts when an iron artifact has its protective concretion accidentally removed during archaeological excavations testifies to the effect of such activities (MacLeod, 1987).

Another shipwreck subjected to explosives during salvage operation was *Pareora* (1919), which shows an elevation of some six percent. Most of the blasting on this site took place during initial salvage operations, and much of the effect also could be due to stresses imparted to the vessel during blasting operations. In contrast, most of the blasting on *Clan Ranald* took place some 50 years after the vessel had foundered. Clearly, the effect of stripping of the protective concretion has a much larger effect on the vessel after the iron has been subjected to decades of corrosion activity.

Trawling Operations in Closed Waters

Shortly after the initial in situ corrosion survey of the Australian wreck *City of Launceston* (1865) in Port Phillip Bay in Victoria, a moratorium was placed on scallop dredging. The site is still littered with the remains of scallop dredges that became entangled with the wreck. *City of Launceston* lies on a shingle bottom, surrounded by a silt mound several meters deep at the midpoint of both port and starboard sides of the hull, but the vessel is still intact. The primary reason for the dredging ban was the diminishing resource (local fishermen were not staying within the bag limits imposed by the Fisheries Department). The presence of the wreck and the damage the fishermen were doing had no effect on the enactment of the ban.

When the site was reassessed six-plus years later, it was noted that the apparent corrosion rate had fallen by approximately 21 percent, and that the extent of marine growth was much greater than it had been during the first season. A subsequent set of measurements one year later confirmed that the lowered corrosion rate was maintained. Although the amount of suspended sediments in the bay varies significantly (Cowdell et al., 1985), normal peaks in this indicator occur in the warmer late spring and summer months. Thus, the improved visibility noted in November and December is not simply a reflection of better timing in the cycle of visitation, since November visibility should be expected to be lower than April values. It appears that cessation of dredging this silty bottom sediment has assisted in the support of a more developed marine ecology; this in turn has led to a lowered corrosion rate.

Salinity

Iron's overall corrosion behavior changes markedly with chloride ion concentration but not unduly over the normal range of salinities associated with natural variations in seawater. Once chloride concentration rises above 2 ppm, overall kinetics do not change appreciably until 500 ppm (salinity of 1 ppt), then up to normal seawater at 18,500 ppm or salinity of 35 ppt. In the Great Lakes of Canada and the United States, the corrosion behavior of iron is dominated by the natural alkalinity of fresh water. Although only a few ppm of chloride are present, this amount still corrodes iron objects in much the same way as in Australian riverine systems such as the River Murray, which is 100 times more salty. During a study of submerged barges and paddle steamers in South Australia's River Murray, a gradual increase in salinity from 113 ppm to 520 ppm upstream, to 410 ppm chloride near the river mouth, does not seem to have had a major effect on the corrosion mechanism (MacLeod, 1993b, 1994).

A series of measurements on seven shipwrecks in the Fathom Five National Park of Lake Huron has shown that this approach works as a sensitive indicator of microenvironment for the iron fastenings in this alkaline freshwater lake. Because of the alkalinity, iron fastenings holding together the wooden vessels are covered in dense and thin layers of calcium carbonate (MacLeod, 1999b).

EFFECTS OF METAL COMPOSITION AND RATE OF CONCRETION GROWTH

Analysis of the metal composition of iron objects and the thickness of concretion has shown that there is a direct relationship between thickness of the marine concretion and weight percent of phosphorous in the metal (MacLeod, 1988). If the rate of corrosion is partly dependent on the thickness of the concretion (on the electrical resistivity of that pathway), the artifacts containing a greater percentage of phosphorous might be expected to corrode at a slower rate, owing to the increase of resistance due to a greater concretion thickness. It should be noted that too little data exists to check this supposition readily.

Other biological factors also can be important. An example of this has been found on Norfolk Island, at the wreck site of HMS *Sirius*. One cause for differences in corrosion potential of similar materials appears to lie in the presence of the black long-spined sea urchin, *Heliocidaris tuberculata* (Lamarck, 1816), which burrows into the marine growth on the artifacts, thereby shortcircuiting one rate-determining parameter in the corrosion cell: the electrical resistance of the concretion layer. Inspection of HMS *Sirius*' carronade and ballast pigs' surfaces shows that hemispherical depressions in the cast iron are due to the burrowing of marine organisms.

EFFECTS OF WATER DEPTH ON E_{corr}

A function of the encapsulating concretion that forms on iron objects of a wreck site is to act as a buffer zone between the immediate physical environment of the sea and the artifact. It also serves to separate dissolved oxygen from corroding metal. In the warm tropical to subtropical waters of Australia, marine growth is dominated by coralline algae and bryozoa as primary colonizers. E_{corr} values fell by 21 ± 3 mV/m in both the ocean and in the River Murray (MacLeod 1989a, 1994). Since all the metal was covered with a thin and dense layer of accretion, the physical separation of anode and cathode of the

corrosion cell is similar to that of sea water. The combination of pH and E_{corr} data for 10 riverine sites indicate that pH is controlled by the equilibrium between magnetite, Fe_3O_4 , and Fe^{2+} ions, whereas in sea water it is dominated by the equilibrium between Fe^{2+} and $Fe(OH)_2 \cdot FeCl_2$. In the absence of such dense concretion layers, depth dependence of E_{corr} is less in the cooler waters of Gulf St. Vincent in South Australia, where E_{corr} fell by only 3 mV/m, and in the adjacent Spencer Gulf, where E_{corr} fell by 5 mV/m of water depth (MacLeod, 1998).

VOLTAGE DIFFERENCES BETWEEN WROUGHT AND CAST IRON

Correct interpretation of corrosion potentials requires that the measurements relate to the same type of metal in the same chemical environment. If this is not the case, errors of interpretation most likely will occur. Since all the forms of iron encountered on a wreck site have corroded in an essentially similar fashion, it is possible to interpret the data with a reasonable degree of confidence. Although iron artifacts are often difficult to conserve because of the way in which chloride ions have permeated the metal's microstructure, collections of hull plates, boilers, cast iron fittings, and anchors all behave in similar fashion. Under conditions generally found on the seabed, iron corrodes in a film-free state in an active corrosion zone of the Pourbaix diagram (Pourbaix, 1974). Thus, a more anodic voltage is a measure of an increased corrosion rate, whereas if the metal was in a passive state with a protective film over the metal, the reverse could be the case. However, in the initial study of the effects of water depth on E_{corr} on the HMS *Sirius* site, such complications were not present, and systematic differences in E_{corr} between wrought and cast iron of approximately 70 mV occurred at the same water depth (MacLeod, 1989). More anodic voltages of cast iron are due to the much higher carbon content of cast iron. Since the graphite form of carbon in the microstructure of alloys is inert, cast iron objects have less negative E_{corr} values, yet corrode at the same rate as wrought iron fittings at 70 mV more cathodic voltages.

With less dense layers of marine growth on the surface of the corroded iron objects, such as in South Australian waters, separation between the characteristic voltages of cast iron and wrought iron are less and vary between 12 mV and 20 mV, depending on the local site differences in marine biology and overall physical oceanography. Clearly, less dense concretions do not support such a large diffusion gradient in pH. They also provide less of a physical barrier to oxygen. In turn, this leads to less of a differentiation between carbon-rich and lower carbon sources in cast iron and wrought iron objects. For similar water depths and similar chemical microenvironments, cast iron fittings will have higher, less negative E_{corr} values than corresponding wrought iron and steel objects.

EFFECT OF ARCHAEOLOGICAL ACTIVITY ON LATER CORROSION OF RESIDUAL DEPOSITS

Analysis of corrosion data collected in the predisturbance survey of the *Xantho* site led to the installation of aluminium sacrificial anodes on the engine and propeller shaft (MacLeod et al., 1986) to minimize further corrosion damage. During recovery operations, corrosion potential measurements were used to gauge the effect of excavation on the stern's remaining parts. The quantification of the differences in E_{corr} values observed during the various stages of archaeological intervention on the site can be made

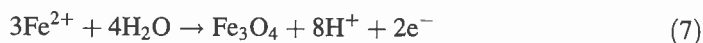
with the knowledge that a tenfold increase or decrease in corrosion rate is indicated by a 370 mV change in the value of E_{corr} (See Section 5.1. Dissolved Oxygen). The data show that application of anodes to the propeller shaft caused a 37 percent reduction in the corrosion rate of the drive train. At the end of the life of the anode in May 1986, the corrosion rate had increased by 14 percent above the predisturbance level, or a 57 percent increase above the previously protected level. This clearly indicates that the removal of the engine did have an initial adverse effect on the corrosion rate of downstream areas. The attachment of new anodes in 1986 caused the predisturbance corrosion rate to be cut in half. The E_{corr} of the stern plating increased to 48 mV four days after the removal of the engine, which indicated an increased degree of water turbulence; this amounts to a 35 percent increase in corrosion rate.

Although the relative corrosion rate for the stern section fell by 12 percent after a year, as increased sand coverage began to correct the effects of the engine removal, it was not until new anodes were attached directly to the stern section that the initial effect of archaeological intervention was corrected. The stern section's present condition is that the corrosion rate has been reduced by 91 percent compared with predisturbance values (MacLeod, 1998b).

CORROSION POTENTIALS AS AN IDENTIFICATION TOOL IN ZERO-VISIBILITY CONDITIONS

River Murray was the major trading route for much of the inland areas of Victoria and South Australia in the 19th century. One consequence of this extensive riverine traffic was the deposition of a substantial number of submerged and partially submerged wrecks over a period of many decades. Since the river's turbid waters preclude visual inspection methods, a study of the corrosion potentials of metals on the sites can act as a set of sensitive "remote sensing" eyes. It is proposed to use E_{corr} measurements as a database for monitoring changes in site conditions; this is the first time corrosion data has been used for this purpose under "black water" conditions. E_{corr} data was recorded on board the support vessel and communications were via a tethered life line and "comms" setup. Voltages were read on board, and the diver was instructed to hold the electrodes in particular configurations once good electrical contact was made. The electrodes were connected with 15-m lengths of insulated cable clipped to the lifeline to keep them from becoming snagged on the wrecks, submerged trees, and other debris.

By plotting the average corrosion potentials for the iron frames and engine components from different sites on a Pourbaix diagram, it is easy to see the varying degrees of corrosion activity that characterized each site. The average E_{corr} values for all sites where solid metal is present show that all the wrecks are in the region of active corrosion. Equilibrium reactions appear to be related to the corrosion of iron to produce Fe^{2+} ions, which are in equilibrium with magnetite, Fe_3O_4 according to the following reactions 6 and 7:



The pH of the microenvironment associated with this equilibrium is given by the relationship

$$E^0 = 0.980 - 0.2364 \text{ pH} - 0.0886 \log[\text{Fe}^{2+}] \quad (8)$$

which for the pH of 6.46 observed on the concreted sections on *Uranus* at Goolwa gives a ferrous ion concentration of $3.9 \times 10^{-5} \text{ M}$ or roughly 2.2 ppm Fe^{2+} in equilibrium with magnetite. All these data are consistent with a slow corrosion rate. Assuming that this pH value is typical, average corrosion potentials on *Jolly Miller* correspond to approximately 200 ppm Fe^{2+} ions in the immediate vicinity of the corroding metal.

Some individual E_{corr} measurements on the extensively corroded iron materials of *William Randell* and *Cobar* are in the region where FeOOH is the stable form of iron. These data also are consistent with the observation that the fittings appeared to be extensively degraded and that there is essentially no solid metal remaining in them. The diver indicated several times that he believed the solid iron-stained beams were "real," but the voltage measurements were typical of iron (III) corrosion products such as FeOOH impregnated into wooden timbers. Thus, the E_{corr} measurements confirmed the presence of wooden beams on the *J.G. Arnold*, *William Randell*, and *Ventura* sites. Since many areas of the river have iron wrecks and wooden wrecks on the same spot, such measurements are a vital part of determining what part of the site belongs to a particular wreck.

A summary of average corrosion potentials for iron fittings and iron structural material on the vessels is found in Table 41.1. Only one of each of the pairs of vessels at each of the main sites at Goolwa, Morgan, and Waikerie is listed, since they all had similar corrosion potentials. Where the vessels were at a similar depth, the more corrosive environments closely correlated with increased water flow over those wrecks. More negative E_{corr} values for the vessels upstream of Waikerie, Loxton, and Berri are dominated by greater water depth. Burial in the silt mounds on the site of *Jolly Miller* gave partly-buried iron fittings an E_{corr} 82 mV more negative than values obtained on similar iron sections floating above the river bed. Any parameter that increases water movement in the area of the wrecks will increase the rate of deterioration of metals. Banning water skiing would help the wrecks by removing the effects of the wash from speed boats.

USE OF IN SITU CORROSION STUDIES TO DETERMINE ORIGINAL METAL THICKNESS

Maritime archaeologists often are presented with the problem of trying to determine the nature of the vessel from measurements of original metal thickness, since records often denote the construction details of ribs, frames, and metal plate thickness. In the past, this

Table 41.1. Corrosion parameters for iron and wooden wrecks in River Murray, South Australia.

Wreck	Miles from Sea	Town	Cl ppm	pH (river)	E_{corr} volts vs. NHE
<i>Uranus</i>	5	Goolwa	410	7.90	-0.163 ± 0.007
<i>Crowie</i>	199	Morgan	185	7.86	-0.150 ± 0.019
<i>J.G. Arnold</i>	224	Waikerie	168	7.67	-0.229 ± 0.025
<i>Jolly Miller</i>	298	Loxton	154	7.67	-0.282 ± 0.033

was estimated by using the preserved form of the object encapsulated in the calcareous concretion. This approach has great limitations, not the least of which is that the method is essentially destructive: It involves smashing open and cleaning out the concretions. A novel way to use in situ corrosion data to estimate the original metal thickness of such fittings is to use a combination of residual metal thickness and an estimate of amount of metal lost from the time of shipwreck.

Residual metal thickness data can be obtained using devices such as a Cygnus digital meter, which provides a readout of the solid metal retained in the structure. Once a site-specific corrosion equation has been established for a wreck site, this relationship can be used to determine total amount of metal lost during the time of immersion in seawater. An example of this approach was used initially on the wreck of HMVS *Cerberus* to establish the method, since the original specifications were at hand. The corrosion equation for the site is given by the relationship shown in Equation 9:

$$\log d_g = 3.29E_{corr} + 0.286 \quad (9)$$

This equation can then be used to determine what the current E_{corr} data corresponds to in terms of how fast the metal is corroding, expressed in terms of mm/year of immersion.

Data on residual metal thickness presented a large spread, from 20 mm to as low as 3 mm, along the length of the vessel and between the upper works to the bottom of the vessel. Ultrasonic metal thickness measuring devices report on the thickness of solid metal bounced back from the interface between solid metal and degraded material. Given that the original armor plating was between 8–10 in (203–254 mm), it is readily apparent that our experimental method did not pick up massive plating, and that data related to an outer zone of metal that lay on top of the original armor. The supposition that the outer upper skin was an addition that took place after construction was shown to be correct: Inspection of the wreck's starboard side shows a clear line of extra plating that ends about 3 m below the original deck height. It is apparent that the data relates to secondary cladding over the armor belt and to the degraded values of plating and frames and ribs.

When thickness data is plotted in order of increasing residual material, four subsets of solid metal thickness appear. The data, summarized in Table 41.2, indicated that *Cerberus* used a range of metal thicknesses which generally was incremented by 1/8 in and that the vessel's upper works have suffered greater corrosion than the middle. The amount of corrosion of the upper section is similar to that of the frames and ribs at the interface between the sea bed and the vessel.

The implications of this study for underwater heritage managers are significant. Field measurements of residual metal thickness, in association with on-site depth of corrosion data from cast iron, can provide a method of determining the original dimensions of the scantlings. Many wrecks contain only a series of iron ribs and frames,

Table 41.2. Average metal thickness for iron on the HMVS *Cerberus* site.

Mean thickness (mm)	Corrosion loss (mm)	Calculated original (mm or in)	Number of samples
3.77 ± 0.46	8.9	12.7 mm or 1/2 in	23
7.60 ± 0.79	8.3	15.9 mm or 5/8 in	16
11.7 ± 0.95	7.4	19.1 mm or 3/4 in	7
18.2 ± 2.40	8.8	27.0 mm or 1 ¹ / ₁₆ in	7

which could have come from a number of vessels known to have been lost in the general vicinity. Given that most wrecks at the same site came from different-sized vessels and from different periods of history, this new approach of using the corrosion measurements as a diagnostic tool has major implications for maritime archaeology.

The method has been applied to the wreck of *Clan Ranald* (1909) in South Australia to determine the original specifications for the thickness of the donkey boilers and the main boilers, since this data was not to be found among Lloyd's specifications or among the ship's drawings. The method accurately determined the correct scantling thicknesses as laid down in the Lloyd's tables for turret-style vessels (MacLeod, 1998a).

IN SITU CONSERVATION OF CORRODED IRON OBJECTS

A number of treatments have been performed on extensively corroded iron objects using sacrificial anodes to reverse the effect of hundreds of years of corrosion from the effects of dissolved oxygen in aggressive site conditions. Although experiments are currently underway on the site of *Swan* (1653) in Scotland and *Resurgam* (1867) off the Welsh coast (Gregory, 1998; MacLeod, 1999), the only completed works have been done on materials recovered from the wreck of HMS *Sirius* (1790) on Norfolk Island in the South Pacific Ocean.

HMS *Sirius* bow anchor

A section of concretion cover was accidentally removed from the shank of the bow anchor during excavation. The concomitant increased corrosion rate was monitored four days before the decision was made to attach an anode. After a year of treatment with an aluminium anode, the area of concretion loss was covered by a calcareous scar (MacLeod, 1987). If 50 percent current efficiency is assumed, the loss of 7 kg of anode material should have provided complete cathodic protection (Fischer, 1983). The effectiveness of the treatment can be gauged from the final E_{corr} value of -0.430 volts vs the Normal Hydrogen Electrode (NHE), which has an equivalent pH of 7.43, assuming the surface is in equilibrium with hydrogen discharge. Copious amounts of hydrogen escaped when the concretion was cracked at the end of the treatment program. The increase from a pH of 5.6 to 7.4 indicates a major reduction of hydrogen ion activity as a result of the cathodic current flowing into the anchor. The other principal effect of the cathodic current is that chloride ions diffuse through the concretion into the surrounding sea water (MacLeod, 1988).

After being removed from the sea, the anchor was given follow-up treatment of gentle electrolysis for over two years. On final examination, the anchor was shown to have retained large areas of the original surface (Carpenter, 1986; MacLeod, 1989). The normally encountered friable surface that characterizes zonal corrosion of wrought iron was replaced by a solid but fragile matrix (Chilton and Evans, 1955). The best-preserved surfaces were those that had suffered no damage to the concretion during the excavation process. One of the main reactions that probably takes place under the concretion layer is the electrochemical reduction of iron (III) corrosion products to form magnetite and hydrogen, as shown in Equation 10:

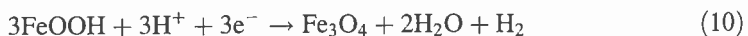


Table 41.3. Corrosion parameters for the HMS *Sirius* carronade.

Date	E_{corr} volts vs. NHE	pH	Object condition
10/15/88	-0.240	5.82	Predisturbance
10/24/88	-0.379	not measured	anode attached
3/20/90	-0.300	7.16	anode lost
3/26/90	-0.485	8.19	anode attached

In the absence of corrosion, and under the influence of cathodic current, chloride ions will diffuse out of the matrix. The reduction in acidity will tend to promote redeposition of calcium/magnesium carbonates (magnesium calcites) and deposition of the iron carbonate siderite (FeCO_3). Slag inclusions are retained in a complex matrix, which results in replication of surface detail, such as manufacturing stamps. The one year of pretreatment was equivalent to one year of land-based treatment.

HMS *Sirius* Carronade

Following the successful treatment of the anchor, a similar approach was applied to the second *Sirius* carronade (Stanbury, 1994). Predisturbance data and three other measurements over three years led to a much clearer understanding of the changes that occur during seabed electrolysis. Predisturbance data showed that the gun was in a highly corrosive microenvironment, hardly surprising since the gun lay in 1.5 m of water in the full surf zone on top of a reef platform. Treatment progress can be seen by the changes in the E_{corr} values and pH (Table 41.3).

On connecting the first anode, the 140 mV decrease toward more negative potentials showed that good electrical contact had been made and that the cathodic current was flowing into the carronade. It was necessary to replace the first anode because of a violent storm, which moved a 1.5 ton concrete plinth several hundred meters across the seabed and ripped the first anode from the carronade (Henderson, 1989).

After three more years of cathodic protection, the carronade was excavated from the depression in the reef and freed from the encapsulating coral. During the excavation process, some of the concretion was accidentally dislodged from the breech end at the cascable. Despite this direct exposure to oxygenated sea water, there was no sign of flash rusting during the final four days of excavation work, indicating clearly that the carronade had undergone significant stabilization. Although the final E_{corr} was measured, a sudden deterioration in site conditions precluded recording pH. If pH is in equilibrium with hydrogen at the same voltage as the corrosion potential, it can be seen that the calculated final pH of 8.2 is the same as the surrounding sea water, which means the treatment was essentially complete. During excavation, large volumes of gas evolved from small fissures in the concretion layer, which is consistent with hydrogen evolution. The alkalinity and lowered chloride content of the metal both increase the degree of safety for recovery and transport to conservation facilities for the extensively degraded object.

The carronade was deconcreted eight months after recovery, revealing a wooden tompion that had kept the bore sealed for 200 years. The tompion's inner surface was covered with a brown, waxy-oily layer containing elemental sulphur, which probably came

from gun powder residues. A massive ball of wadding was attached by a rope to the tompon; the organic materials were quickly treated with neutral citrate solutions to prevent damage due to oxidation and precipitation of iron corrosion products (MacLeod et al., 1991).

The total amount of chloride removed during the laboratory phase of the treatment of the carronade was 4.22 kg, a small amount indicating that a significant mass of chloride had been removed during in situ treatment. Since it was not possible to determine directly the initial amount of chloride removed, it was necessary to resort to a series of comparative measurements in order to estimate the efficiency of the treatment.

The first method involves a comparison of the composition of the *Sirius* bore solution and the bore solution from a similarly plugged gun from the wreck of *Zuytdorp* (1712). The chloride ion concentration of the 1.4 liters of bore solution trapped by the tompon gave a concentration of 8366 ppm, less than half the amount of chloride ions found in local sea water. Thus the chloride ions had diffused through the concretion into the sea. Given that the *Sirius* gun had corroded for only 200 years compared with 275 years for *Zuytdorp*, the initial chloride content of 54,593 ppm found inside the bore of the *Zuytdorp* gun may have been as high as $54,593 \times (200/275)$ or some 39,704 ppm in the *Sirius* ordnance. This may mean pretreatment reduced chloride levels in the bore solution by 78.9 percent during the time on the seabed.

A second way of estimating amount of chloride released is to compare mass losses of the two HMS *Sirius* carronades. The first carronade, SI 58, suffered a weight loss of 26.88 percent with a corrosion depth of 25 mm, while the second carronade lost only 20.7 percent but had a much greater depth of corrosion, at 39.5 mm. Since the guns have the same shape, it is reasonable to assume that, with an open bore, the mass loss from corrosion should be related directly to their depths of corrosion. After correcting for immersion of five years longer for the second gun, the calculated mass loss might have been expected to be $(200/195) \times 39.5/25 \times 26.8\text{wt percent}$ or 43.4 percent. This figure may seem extraordinarily high, but a cast iron ballast pig from the same part of the wreck site as the second carronade lost 57.9 percent of its weight for a corrosion depth of 35.5 mm. Another ballast pig, with a corrosion depth of only 27.6 mm, had lost 43.8 percent of its original weight.

Details of the methods for calculating original chloride content of the carronade can be found in the primary reference, but the data indicates that somewhere on the order of 80 percent of the chlorides were removed before excavation (MacLeod, 1996b). Typical surface chloride activity measurements on freshly exposed marine iron artifacts are of the order 40,000 ppm chloride, whereas the surface under the concretion layer was 4100 ppm immediately after the recovery of the gun. Surface chloride activity fell to only 0.4 ppm at the end of the two years of electrolysis, which showed the treatment was finished.

GLOSSARY

ppm: Parts per million or $\mu\text{g}/\text{gram}$

ppt: parts per thousand

PDB: PeeDeeBelemite. PDB is the acronym for the mineral that is a reference sample of a Cretaceous belemnite, *Belemnitella americana*, from the Pee Dee formation in South Carolina. The carbon dioxide evolved from the reaction of the limestone, with 100 percent phosphoric acid at 25.2°C, is used as a standard in carbon isotope measurements for determining $^{13}\text{C}/^{12}\text{C}$ ratios. Details are found in Craig, 1957.

REFERENCES

- Carpenter, J., 1986, *Conservation of an Anchor from the Wrecksite of HMS Sirius (1790)*. Unpublished report, Australian Bicentennial Authority.
- Carpenter, J., and MacLeod, I.D., 1993, Conservation of Corroded Iron Cannon and the Influence of Degradation on Treatment Times. *ICOM-Committee for Conservation, Preprints 10th Triennial Conference*, Washington, D.C., Vol. II, pp. 759–766.
- Chilton, J.P., and Evans, U.R., 1955, Corrosion Resistance of Wrought Iron. *Journal of the Iron and Steel Institute*, 113–122.
- Cowdell, R.A., Gibbs, C.F., Longmore, A.R., Theodoropolous, T., 1985, *Tabulation of Port Phillip Bay Water Quality Data between June 1980 and July 1984*. Internal Report No. 98, Marine Science Laboratories, Ministry for Conservation, Fisheries and Wildlife Division, Queenscliff, Victoria.
- Craig, H., 1957, Isotopic Standards for Carbon and Oxygen and Correction Factors for Mass-spectrometric Analysis of Carbon Dioxide. *Geochimica et Cosmochimica Acta* 12:133–149.
- Ellett, D.J., and Edwards, A., 1983, Oceanography and Inshore Hydrography of the Inner Hebrides. *Proceedings of the Royal Society of Edinburgh* 83B:143–160.
- Fischer, K.P., 1999, *Microbial Corrosion*. Metals Society, London.
- Gregory, D., 1999, Monitoring the Effect of Sacrificial Anodes on the Large Iron Artifacts on the Duart Point wreck, 1997. *International Journal of Nautical Archaeology* 28(2): 164–173.
- _____, 2000, In situ Corrosion on the Submarine *Resurgam*: A Preliminary Assessment of Her State of Preservation. *Conservation and Management of Archaeological Sites Volume 4* pp. 93–100.
- Henderson, G., and Henderson, K.J., 1988, *Unfinished Voyages 1851–1880*, p. 57. University of Western Australia Press, Nedlands.
- Henderson, G.J., 1989, *1988 Expedition Report on the Wreck of HMS Sirius (1790)*. Unpublished report to the Australian Bicentennial Authority, pp. 1–95.
- Hunt, J.M., 1979, *Petroleum Geochemistry and Geology*. W.H. Freeman, San Francisco, p. 178.
- Kimpton, G., and McCarthy, M., 1988, The Freeing of the SS *Xantho* engine. In *Papers from the First Australian Institute for Management of Iron Ships and Steam Ship Wrecks*, edited by M. McCarthy, pp. 73–74. Australian Institute for Maritime Archaeology Conference Series No. 1.
- Kiss, L., 1988, *Kinetics of Electrochemical Metal Dissolution, Studies in Physical and Theoretical Chemistry*, Vol. 47, p. 60. Elsevier, Oxford.
- La Que, F.L., 1975, *Marine Corrosion*. John Wiley and Sons, New York.
- Lenihan, D.J., 1989, *Submerged Cultural Resources Study, USS Arizona Memorial and Pearl Harbor National Historic Landmark*. Southwest Cultural Resources Center Professional Papers No. 23, pp. 1–192, Santa Fe.
- MacLeod, I.D., 1981, Shipwrecks and Applied Electrochemistry. *Journal of Electroanalytical Chemistry* 118:291–304.
- _____, 1982, Formation of Marine Concretions on Copper and Its Alloys. *International Journal of Nautical Archaeology & Underwater Exploration* 11(4):267–275.
- _____, 1986, Conservation of the Steamship *Xantho*. *ICCM Bulletin* 12(3/4):66–94.
- _____, 1987, Conservation of Corroded Iron Artifacts: New Methods for on-site Preservation and Cryogenic Deconcreting. *International Journal of Nautical Archaeology* 16(1):49–56.
- _____, 1988, Conservation of Corroded Concreted Iron. *Proceedings of Conference 28*, Australasian Corrosion Association, Perth, pp. 2–6.1, 2–6.9.
- _____, 1989a, Electrochemistry and Conservation of Iron in sea Water. *Chemistry in Australia* 56(7):227–229.
- _____, 1989b, Marine Corrosion on Historic Shipwrecks and Its Application to Modern Materials. *Corrosion Australasia* 14(3):8–14.
- _____, 1989c, The application of corrosion science to the management of maritime archaeological sites. *Bulletin of the Australian Institute for Maritime Archaeology* 13(2):291–304.
- _____, 1992, Conservation Management of Iron Steamships: The SS *Xantho* (1872). *Transactions of Multi-Disciplinary Engineering GE* 16(1):45–51.
- _____, 1993a, Metal Corrosion on Shipwrecks: Australian Case Studies. *Trends in Corrosion Research* 1:221–245.
- _____, 1993b, Conservation Assessment.” In *Historic Shipping on the River Murray. A guide to the terrestrial and submerged archaeological sites in South Australia*, edited by Sarah Kenderdine, pp. 273–282. State Heritage Branch, Department of Environment and Land Management, Adelaide.

- _____, 1994, Report on the Corrosion of Iron Shipwrecks in South Australia with Particular Reference to the River Murray. In *Muddy Waters: Proceedings of the First Conference on the Submerged and Terrestrial Archaeology of Historic Shipping on the River Murray*, Echuca, September 1992, pp. 1–14. State Heritage Branch, South Australia Department of Environment and Natural Resources, Adelaide.
- _____, 1995, In situ Corrosion Studies on the Duart Point Wreck 1994. *International Journal of Nautical Archaeology* 24(1):53–59.
- _____, 1996a, An in situ study of the corroded hull of HMVS *Cerberus* (1926). *Proceedings of the 13th International Corrosion Congress*, Paper 125:1–10.
- _____, 1996b, In situ Conservation of Cannon and Anchors on Shipwreck Sites. In *Conservation of Archaeological Sites and Its Consequences*, IIC, edited by Ed Ashok Roy and Perry Smith, pp. 111–115. London.
- _____, 1998a, In situ Corrosion Studies on Iron and Composite Wrecks in South Australia Water: Implications for Site Managers and Cultural Tourism. *Bulletin of Australian Institute of Maritime Archaeology* 22:81–90.
- _____, 1998b, In situ Corrosion Studies on Iron Shipwrecks and Cannon: The Impact of Water Depth and Archaeological Activities on Corrosion Rates. In *Metal 98 Proceedings of the ICOM—CC Metals Working Group Conference*, edited by W. Ed Mourey and L. Robbiola, Draguignan-Faginere, France 1998, James & James, London pp. 116–124.
- MacLeod, I.D., and North, N.A., 1980, 350 years of marine corrosion in Western Australia. *Corrosion Australasia* 5:11–15.
- _____, 1987, *Corrosion of Metals*. In *Conservation of Marine Archaeological Objects*, edited by C. Pearson Butterworths, pp. 68–72. London.
- MacLeod, I.D., North, N.A., and Beegle, C.J., 1986, The Excavation, Analysis and Conservation of Shipwreck Sites. In *Preventative Measures during Excavation Site Protection*. ICCROM Conference, Ghent, 1985, pp. 113–131.
- MacLeod, I.D., Brooke, P., and Richards, V.L., 1991, Iron Corrosion Products and Their Interactions with Waterlogged Wood and PEG. *Proceedings of the 4th ICOM Group on Wet Organic Archaeological Materials Conference*, Bremerhaven, 1990, edited by Per Hoffmann, pp. 119–132.
- McCarthy, M., 1988, SS *Xantho*: The Pre-disturbance, Assessment, Excavation and Management of an Iron Steam Shipwreck off the Coast of Western Australia. *International Journal of Nautical Archaeology and Underwater Exploration* 17(4):339–347.
- Martin, C.J.M., 1995, The Cromwellian shipwreck off Duart Point, Mull: An Interim Report. *International Journal of Nautical Archaeology* 24(1):15–32.
- Microbial Corrosion, 1983, *Proceedings of the Conference Sponsored and Organised Jointly by the National Physical Laboratory and the Metals Society and held at NPL Teddington 8–10 March 1983*. The Metals Society, London.
- North, N.A., 1976, The Formation of Coral Concretions on Marine iron. *International Journal of Underwater Archaeology and Underwater Exploration* 5:253–258.
- _____, 1982, Corrosion Products on Marine Iron. *Studies in Conservation* 27:75–83.
- _____, 1989, Proximity corrosion in Seawater. *Corrosion Australasia* 14(5):8–11.
- North, N.A., and Pearson, C., 1978, Recent Advances in the Stabilisation of Marine Iron. In *Conservation of Iron Objects Found in a Salty Environments*, pp. 26–38. Chief Conservators Office. Historical Monuments Documentation Centre, Warsaw.
- Pourbaix, M., 1974, *Atlas of Electrochemical Equilibria in Aqueous Solutions*, 2nd edition. NACE, Houston.
- Rhead, E.L., 1945, Chemical Reactions of Blast furnaces. In *Metallurgy*, pp. 148–150. Longmans, London.
- Riley, J.P., and Skirrow, G., editors, 1975, *Chemical Oceanography, Vol.1*. Second Edition, Academic Press, London.
- Sequeira, C.A.C., and Tiller, A.K., editors, 1988, Microbial Corrosion. In *Proceedings of the First European Federation of Corrosion Workshop on Microbial Corrosion*. Elsevier Applied Science, London.
- Stanbury, M. 1994, HMS *Sirius* 1790. *An Illustrated Catalogue of Artifacts Recovered from the Wreck Site at Norfolk Island*. Australian Institute of Maritime Archaeology Spec. Pub. 7:74–78.
- Strommel, H., Stroup, E.D., Reid, J.L., and Warren, B.A., 1973, Transpacific Hydrographic Sections at Lats. 43°S and 28°S: The *Scorpio* Expedition—I Preface. *Deep Sea Research* 20:1–7.